NASA/TM–2020–5002153

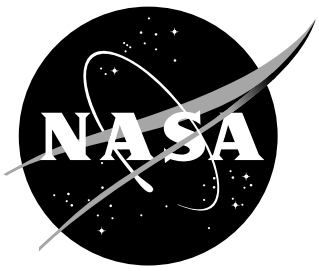

Hover Validation and Acoustic Baseline Blade Set Definition

Austin D. Overmeyer, Peter A. Copp
U.S. Army Army Combat Capabilities Development Command
Aviation & Missile Center
NASA Langley Research Center, Hampton, Virginia

Norman W. Schaeffler
NASA Langley Research Center, Hampton, Virginia

May 2020

NASA STI Program . . . in Profile

Since its founding, NASA has been dedicated to the advancement of aeronautics and space science. The NASA scientific and technical information (STI) program plays a key part in helping NASA maintain this important role.

The NASA STI Program operates under the auspices of the Agency Chief Information Officer. It collects, organizes, provides for archiving, and disseminates NASA's STI. The NASA STI Program provides access to the NTRS Registered and its public interface, the NASA Technical Reports Server, thus providing one of the largest collections of aeronautical and space science STI in the world. Results are published in both non-NASA channels and by NASA in the NASA STI Report Series, which includes the following report types:

- TECHNICAL PUBLICATION. Reports of completed research or a major significant phase of research that present the results of NASA programs and include extensive data or theoretical analysis. Includes compilations of significant scientific and technical data and information deemed to be of continuing reference value. NASA counterpart of peer-reviewed formal professional papers, but having less stringent limitations on manuscript length and extent of graphic presentations.
- TECHNICAL MEMORANDUM.
  Scientific and technical findings that are preliminary or of specialized interest, e.g., quick release reports, working papers, and bibliographies that contain minimal annotation. Does not contain extensive analysis.
- CONTRACTOR REPORT. Scientific and technical findings by NASA-sponsored contractors and grantees.
- CONFERENCE PUBLICATION.
  Collected papers from scientific and technical conferences, symposia, seminars, or other meetings sponsored or co-sponsored by NASA.
- SPECIAL PUBLICATION. Scientific, technical, or historical information from NASA programs, projects, and missions, often concerned with subjects having substantial public interest.
- TECHNICAL TRANSLATION. English- language translations of foreign scientific and technical material pertinent to NASA's mission.

Specialized services also include organizing and publishing research results, distributing specialized research announcements and feeds, providing information desk and personal search support, and enabling data exchange services.

For more information about the NASA STI Program, see the following:

- Access the NASA STI program home page at ***http://www.sti.nasa.gov***
- E-mail your question to help@sti.nasa.gov
- Phone the NASA STI Help Desk at 757-864-9658
- Write to:
  NASA STI Information Desk
  Mail Stop 148
  NASA Langley Research Center
  Hampton, VA 23681–2199

NASA/TM–2020–5002153

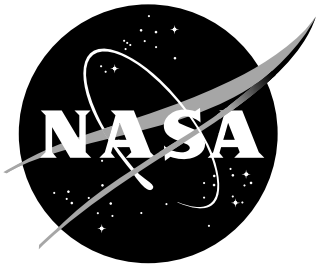

Hover Validation and Acoustic Baseline Blade Set Definition

Austin D. Overmeyer, Peter A. Copp
U.S. Army Army Combat Capabilities Development Command
Aviation & Missile Center
NASA Langley Research Center, Hampton, Virginia

Norman W. Schaeffler
NASA Langley Research Center, Hampton, Virginia

National Aeronautics and
Space Administration

Langley Research Center
Hampton, Virginia 23681-2199

May 2020

Available from:

NASA STI Program / Mail Stop 148
NASA Langley Research Center
Hampton, VA 23681-2199
Fax: 757-864-6500

Abstract

The Hover Validation and Acoustic Baseline (HVAB) blade set has been jointly developed by the U.S. Army Combat Capabilities Development Command Aviation & Missile Center (CCDC AvMC) and the NASA Revolutionary Vertical Lift Technology (RVLT) Project. This Mach-scale, 66.50 *in* radius, blade set will ultimately be tested in both hover and forward-flight to provide key data for analysis validation. This paper provides comprehensive detail of the blade geometry, instrumentation, and structure for use in future analyses.

Contents

List of Figures

List of Tables

Nomenclature

CCDC AvMC	Combat Capabilities Development Command Aviation & Missile Center
HVAB	Hover Validation and Acoustic Baseline
IGES	Initial Graphics Exchange Specification
LED	Light-Emitting Diode
OML	Outer Mold Line
RTD	Resistance Temperature Detectors
RVLT	Revolutionary Vertical Lift Technology
SN	Serial Number
VABS	Variational Asymptotic Beam Sectional Analysis

Symbols

r	Radial Station, $r = X,\ in$
c	Airfoil Chord, in
CG_η	Center of Gravity offset from local η, in
CG_ζ	Center of Gravity offset from local ζ, in
EA	Axial Stiffness, lbf
EI_C	Chord Stiffness, $lbf \cdot in^2$
EI_F	Flap Stiffness, $lbf \cdot in^2$
EI_{FC}	Flap-Chord Stiffness, $lbf \cdot in^2$
GJ	Torsional Stiffness, $lbf \cdot in^2$
I_C	Chord Inertia, $lbf \cdot s^2 \cdot in^2$
I_F	Flap Inertia, $lbf \cdot s^2 \cdot in^2$
I_{FC}	Flap-Chord Inertia, $lbf \cdot s^2 \cdot in^2$
N_b	Number of Blades
R	Rotor Radius, in
SC_η	Shear Center offset from local η, in
SC_ζ	Shear Center offset from local ζ, in
X	Global Blade Radial Axis, +X is toward the tip, in
Y	Global Blade Chordwise Axis, +Y is toward leading edge, in
Z	Global Blade Thickness Axis, +Z is toward the upper surface, in
σ	Rotor Geometric Solidity
η	Local Chordwise Axis, $+\eta$ is toward trailing edge, in
ζ	Local Thickness Axis, $+\zeta$ is toward upper surface, in
$\bar{\eta}$	Tension Center (Neutral Axis) offset from local η, in
$\bar{\zeta}$	Tension Center (Neutral Axis) offset from local ζ, in
θ_c	Collective Pitch, deg
ρA	Sectional Running Weight, $lbf \cdot s^2/in^2$

1 Background Information

1.1 Overview

The Hover Validation and Acoustic Baseline (HVAB) blade set is a Mach-scaled set of rotor blades based on the geometry of the Pressure Sensitive Paint (PSP) blade set, see Refs. [1,2]. A complete description of the PSP rotor blade set is provided as an embedded file, *PSP_Rotor_Definition* (Note: right click on the link to save the embedded file).

The HVAB blade set consists of six blades and is currently under fabrication with an anticipated delivery in June 2020. This document provides the as-designed geometry, instrumentation and structural properties of the HVAB blade set. It is anticipated that a future report will include as-built properties and inspection reports.

1.2 HVAB Blade Set Differences

There are several key differences between the HVAB blade set and the PSP blade set.

1. The rotor radii (66.50 *in*) are identical. The HVAB blades themselves have a larger root cutout to accommodate a larger hub. The root of HVAB blade set starts at 9.30 *in* ($r/R = 0.140$) compared to 7.87 *in* ($r/R = 0.118$) for the PSP blade set.

2. The coincident flap/lag/pitch hinge is located at 3.50 *in* for the HVAB blade set compared to 3.00 *in* for the PSP blade set.

3. The HVAB blades are designed for a trailing edge thickness of 0.0350 *in* compared to the PSP thickness of 0.0300 *in* (both are design values).

4. The HVAB blades have a 0.5 *in* radius at the sweep break located at $r/R = 0.95023$ along the leading edge. The PSP blade set had a sharp break with an undefined radius.

5. The HVAB blade set root fairing (used to cover wiring and connectors) inboard of $r/R = 0.25$ has a slightly different shape than the PSP blade set. The as-designed shape is accurate in the HVAB CAD file.

6. The mass and stiffness properties are significantly different between the two blade sets, due to the large amount of instrumentation in the HVAB blade set.

2 Geometry

2.1 Coordinate Systems

In this report, HVAB geometry data are presented in two different coordinate systems. The global coordinate system is used to define the blade Outer Mold Line (OML). The local coordinate system is used to define the 2D blade structural properties.

The global coordinate system (X,Y,Z), Figure 1, is defined relative to the center of rotation and is independent of blade twist/pitch. The +X is toward the tip, +Y is toward the leading edge and +Z is toward the upper surface.

The local coordinate system (η, ζ) is defined relative to the local airfoil quarter-chord point. The local coordinate system is shown relative to the global in Figures 2(a)-2(b). The $+\eta$ is toward the trailing edge and $+\zeta$ is toward the upper surface. The global coordinate system is shown in black and the local coordinate system is shown in blue. Figure 2(a) shows an example station where a translation is not required and the origin of the local coordinate system lies on the pitch axis (X). Figure 2(b) shows an example where a translation is required and the origin of the local coordinate system is offset from the pitch axis (X).

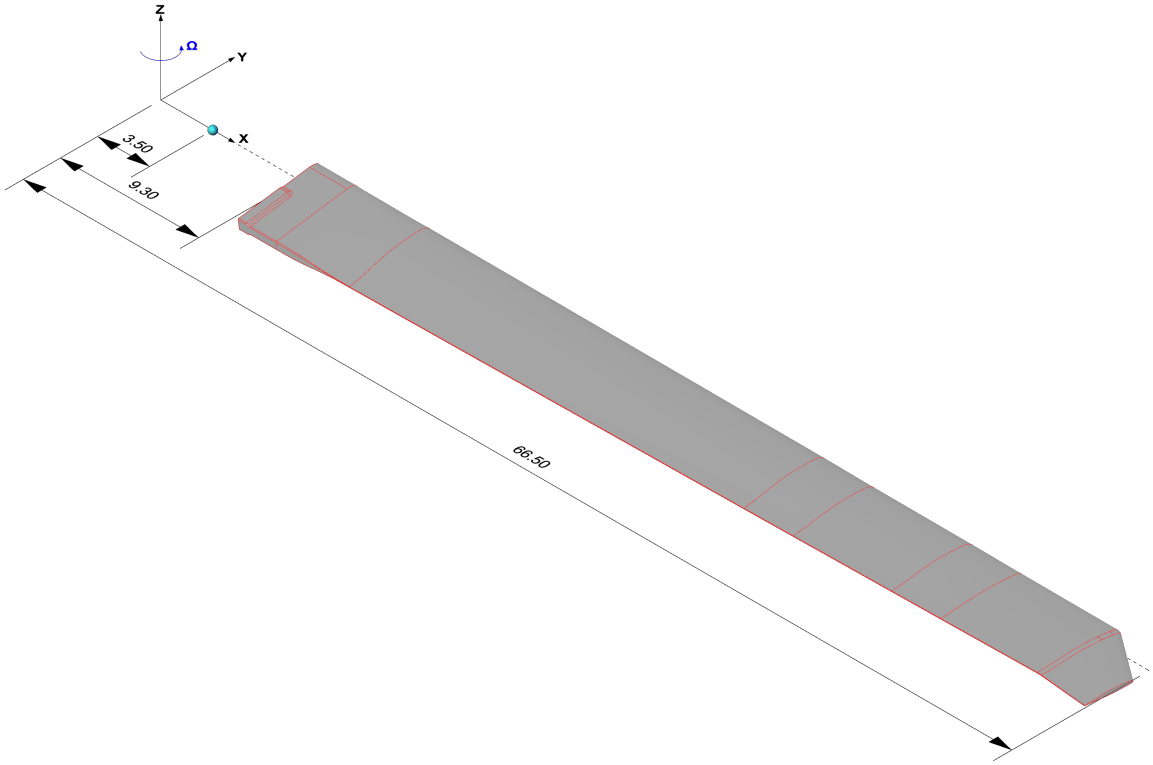

Figure 1. HVAB Global Coordinate System (X, Y, Z).

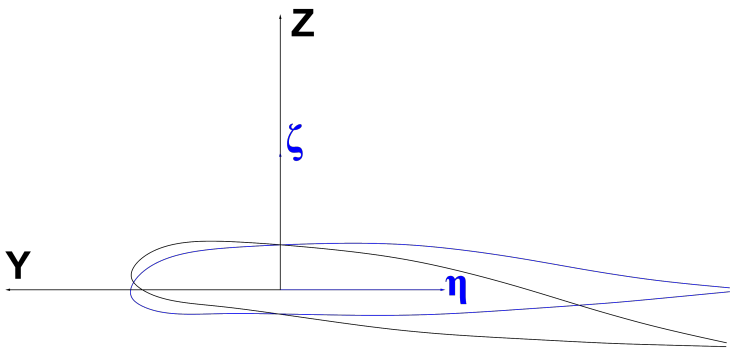

(a) $r/R = 0.25188$

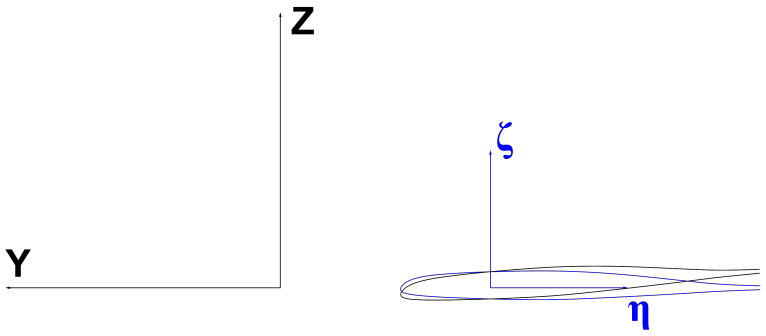

(b) $r/R = 1.00000$

Figure 2. HVAB Local Coordinate System (η, ζ).

2.2 Planform

The general properties of the HVAB planform are provided in Table 1. The chord, twist, sweep, and airfoil distribution are provided in Table 2. A fairing inboard of $r/R = 0.25188$ is used to accommodate wiring and connectors from the instrumentation. The overview planform is shown in Figure 3. The figure also shows the flap-lead/lag hinge to be colocated 3.5 inches from the hub center. The feathering axis is a line coincident with the rotor origin and the flap-lead/lag hinge. The geometric solidity is calculated using Equation 1. The solidity value of 0.1033 assumes there is no root cut out and the root chord of 5.45 inches extends to the center of rotation.

$$\sigma = \int_0^1 \frac{N_b * c(r)}{\pi * R} dr \tag{1}$$

Table 1. HVAB Rotor Blade Characteristics.

Number of Blades, N_b	4
Blade Radius, R (in)	66.50
Blade Chord, c (in)	5.45
Rotor Geometric Solidity, σ	0.1033
Rotor Airfoil	RC series
Blade Twist Distribution	Linear
Blade Twist (deg)	-14

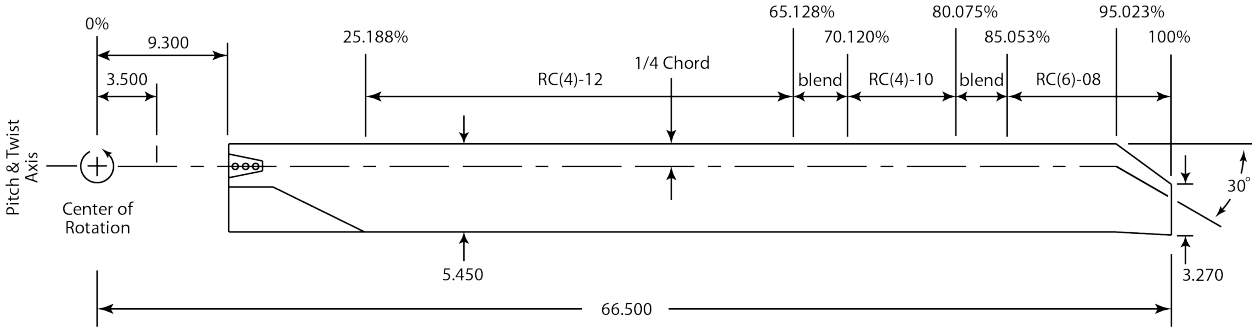

Figure 3. HVAB Planform.

Table 2. HVAB Rotor Blade Planform.

				0.25c Position			
r/R	Twist	c	Sweep	ΔX	ΔY	ΔZ	Airfoil
-	(deg)	(in)	(deg)	(in)	(in)	(in)	-
0.13985	8.20	5.45	0	9.300	0	0	$RC(4)-12$
0.16722	8.20	5.45	0	11.120	0	0	$RC(4)-12$
0.25188	7.01	5.45	0	16.750	0	0	$RC(4)-12$
0.65128	1.40	5.45	0	43.310	0	0	$RC(4)-12$
0.70120	0.70	5.45	0	46.630	0	0	$RC(4)-10$
0.80075	-0.70	5.45	0	53.250	0	0	$RC(4)-10$
0.85053	-1.40	5.45	0	56.560	0	0	$RC(6)-08$
0.95023	-2.80	5.45	0	63.190	0	0	$RC(6)-08$
1.00000	-3.50	3.27	30	66.500	-1.911	0	$RC(6)-08_T$

2.3 Airfoil Coordinates

The blade uses three of the RC-series airfoils that were designed in the early 1990s specifically for rotorcraft applications. The naming scheme for the RC airfoils is RC(X)-YY, where X is the series and YY is the thickness in percent chord. The airfoils are the RC(4)-12, RC(4)-10 [3] and RC(6)-08 [4]. Note that there is not a report available on the RC(4)-12 airfoil. The trailing-edge thickness was modified using PROFIL06 [5] to keep a constant dimensional trailing-edge of 0.035 *in*. The RC(6)-08T was used to designate the thicker nondimensional trailing-edge thickness of the tip airfoil due to the reduced chord. A listing of the final nondimensional airfoil coordinates, scaled by 1000, are embedded in Table 2 (Note: right click on the link to save the airfoil coordinates).

2.4 Outer Mold Line (OML)

The nondimensional airfoil coordinates were scaled by chord, twisted about the local quarter chord then translated to the global coordinate system using the properties provided in Table 2. The blade is provided at collective pitch, $\theta_c = 0$ deg. Collective pitch is defined as the pitch at the $r/R = 0.75$ station.

The outer mold line (OML) of the blade was generated by lofting the provided sections. After lofting the blade from the provided airfoil coordinates, the root fairing area was modified to accommodate the instrumentation and the tip sweep break radius was added. The provided OML captures both of these deviations from the airfoil coordinates. The OML file is provided in Initial Graphics Exchange Specification (IGES) format, and the units are inches. HVAB Blade OML AsDesigned.igs (Note: right click on the link to save the embedded file).

3 Instrumentation

The six blades of the HVAB blade set were instrumented with absolute dynamic pressure sensors, full-bridge strain gauges, resistance temperature detectors (RTD) and light-emitting diodes (LED) for tip tracking. An overview of the number of sensors per type is provided for each blade serial number (SN) in Table 3. The predesign locations, as a function of radius, are shown in Figure 4. The pressure transducer stations on SN004, Hover Blade, are represented by the blue lines. The pressure transducer areas on SN006, Acoustic Blade, are represented by the blue triangles. The strain gauge locations on all blades are represented by the green rectangles. The red squares represent the temperature sensors. The tip LEDs are represented by the purple circles. The as-designed locations are provided in Sections 3.1-3.4.

Table 3. Overview of HVAB Blade Instrumentation.

SN	Type	Strain Gauges	Kulites	RTD	LED
SN001	Standard	3	0	7	1
SN002	Standard	3	0	7	1
SN003	Standard	3	0	7	1
SN004	Hover	3	187	7	1
SN005	Strain	12	0	7	1
SN006	Acoustic	3	51	7	1

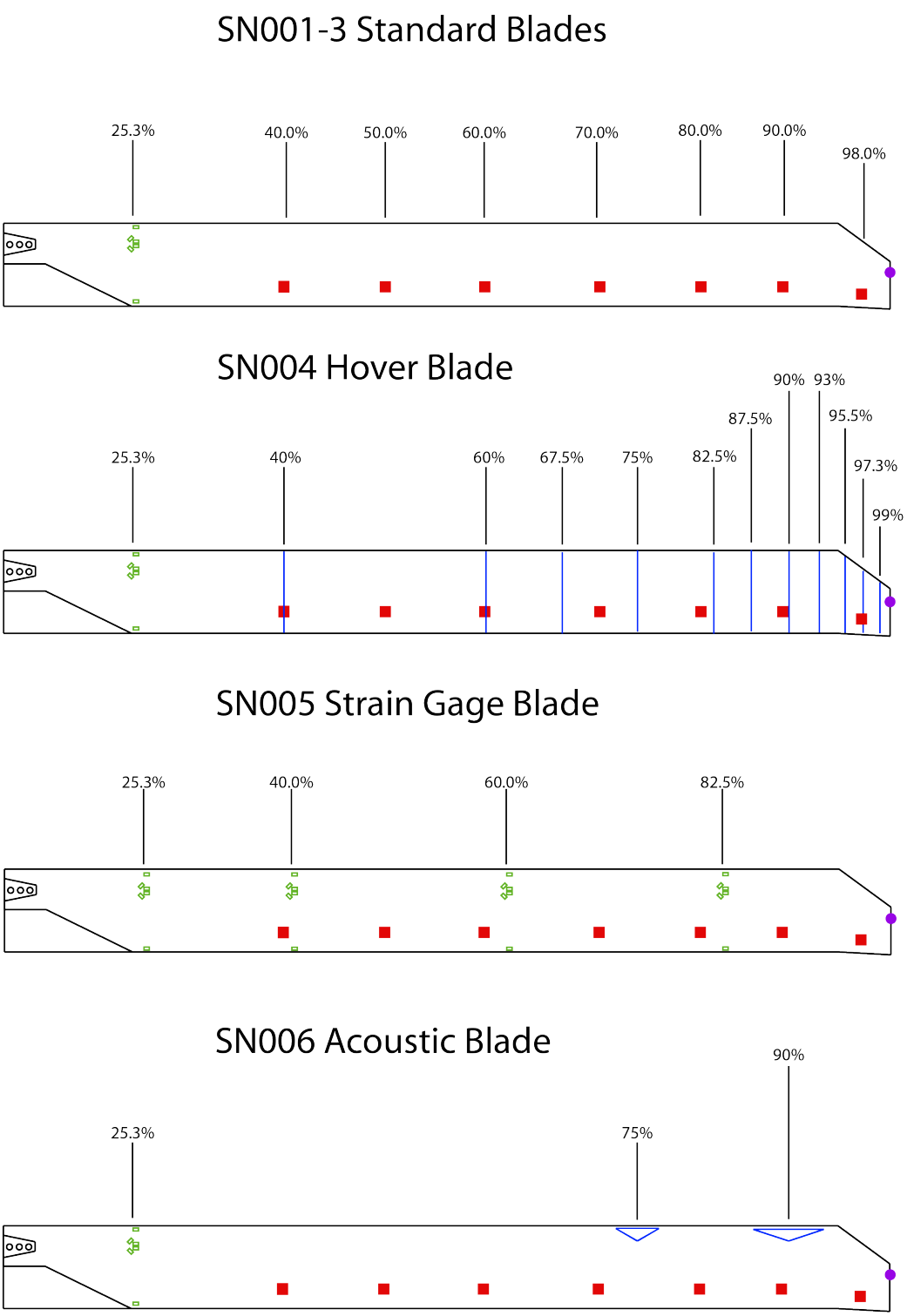

Figure 4. HVAB Predesign Instrumentation Locations.

3.1 Pressure Sensors

The blades SN004 and SN006 were instrumented with absolute dynamic pressure transducers. These transducers were a custom variation on the model LQ-32-064-15A by Kulite Semiconductor Products. The transducers feature temperature compensation modules internal to the transducer housing and are specified by the manufacturer to have a 15 psia range. All of the transducers utilized for this research effort were independently calibrated by the calibration laboratory at the NASA Ames Research Center across a pressure range of 5 to 20 psia and a temperature range of $40°F$ to $120°F$.

3.1.1 Hover Blade, SN004 Pressures

The Hover Blade, SN004, was instrumented with 187 absolute dynamic pressure transducers. The pressure transducers were arranged in 11 stations consisting of 17 transducers each. At each station, there were 11 transducers arranged on the upper surface and 6 transducers along the lower surface. The predesign chordwise locations of the transducers for each radial station were optimized for hover to minimize the error of the integrated coefficients of lift, drag and pitching moments based on discrete transducer locations. The optimization was performed using an extensive set of computed 2D pressure distributions for collective sweeps from 4 to 12-degrees at the design rotor operating condition. As indicated in Figure 4, the predesign locations for the stations, as indicated as a percentage of the radius, were 40%, 60%, 67.5%, 75%, 82.5%, 87.5%, 90%, 93%, 95.5%, 97.3% and 99%.

During the detail design process, some of the station locations were moved slightly to accommodate the blended regions of the planform. Additionally, and more significantly, due to the density of transducers, the physical size of the transducer housing, and space limitations in the blade itself at each station, the upper line of transducers were staggered from the lower line. For a given station, the typical offset between the upper and lower line of transducers was 0.300 inch ($\Delta r/R = 0.0045$). The as-designed nominal station locations, as indicated as a percentage of the radius, were 39.7%, 59.8%, 67.3%, 74.8%, 82.3%, 87.3%, 89.8%, 92.8%, 95.3%, 97.7%, and 98.8%. The as-designed locations for each pressure transducer are presented by station, in both global coordinate system and local coordinate system, nondimensionalized by the local chord, in Tables 4-14. The chordwise locations are shown by the blue circles and plotted on the local nondimensional airfoil for each station in Figures 5-15.

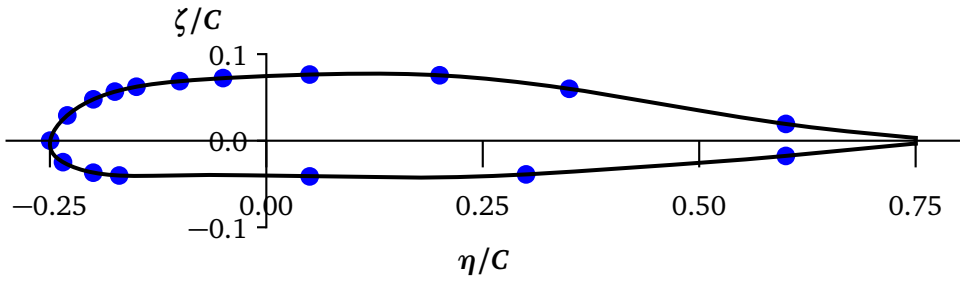

Figure 5. Station 1, Hover Blade - Kulite Locations.

Table 4. Station 1, Hover Blade - Nominal r/R: 0.397, Kulites 1 - 17.

Kulite ID	X (in)	Y (in)	Z (in)	r/R	η/c	ζ/c
1	25.890	-3.249	-0.385	0.389	0.600	-0.018
2	25.890	-1.610	-0.356	0.389	0.300	-0.039
3	25.890	-0.252	-0.248	0.389	0.050	-0.041
4	25.890	0.942	-0.136	0.389	-0.170	-0.040
5	25.890	1.103	-0.104	0.389	-0.200	-0.037
6	25.890	1.287	-0.021	0.389	-0.235	-0.025
7	26.910	-3.268	-0.172	0.405	0.600	0.019
8	26.910	-1.928	0.164	0.405	0.350	0.060
9	26.910	-1.122	0.318	0.405	0.200	0.076
10	26.910	-0.307	0.392	0.405	0.050	0.076
11	26.910	0.238	0.416	0.405	-0.050	0.072
12	26.910	0.511	0.420	0.405	-0.100	0.069
13	26.910	0.786	0.408	0.405	-0.150	0.062
14	26.910	0.924	0.389	0.405	-0.175	0.057
15	26.910	1.063	0.352	0.405	-0.200	0.048
16	26.910	1.235	0.265	0.405	-0.230	0.029
17	26.910	1.356	0.116	0.405	-0.250	0.000

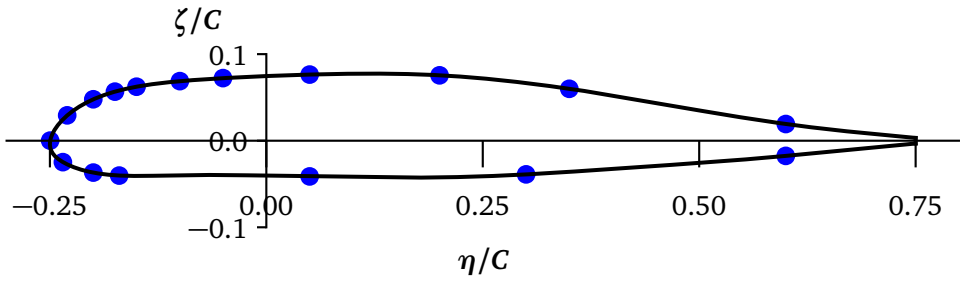

Figure 6. Station 2, Hover Blade - Kulite Locations.

Table 5. Station 2, Hover Blade - Nominal r/R: 0.598, Kulites 18 - 34.

Kulite ID	X (in)	Y (in)	Z (in)	r/R	η/C	ζ/C
18	39.600	1.285	-0.086	0.595	-0.235	-0.025
19	39.600	1.096	-0.159	0.595	-0.200	-0.037
20	39.600	0.934	-0.184	0.595	-0.170	-0.040
21	39.600	-0.264	-0.235	0.595	0.050	-0.041
22	39.600	-1.626	-0.274	0.595	0.300	-0.039
23	39.600	-3.264	-0.220	0.595	0.600	-0.018
24	39.900	-3.272	-0.016	0.600	0.600	0.019
25	39.900	-1.918	0.256	0.600	0.350	0.060
26	39.900	-1.105	0.371	0.600	0.200	0.076
27	39.900	-0.288	0.406	0.600	0.050	0.076
28	39.900	0.258	0.404	0.600	-0.050	0.072
29	39.900	0.530	0.395	0.600	-0.100	0.069
30	39.900	0.804	0.370	0.600	-0.150	0.062
31	39.900	0.941	0.344	0.600	-0.175	0.057
32	39.900	1.079	0.301	0.600	-0.200	0.048
33	39.900	1.247	0.206	0.600	-0.230	0.029
34	39.900	1.360	0.051	0.600	-0.250	0.000

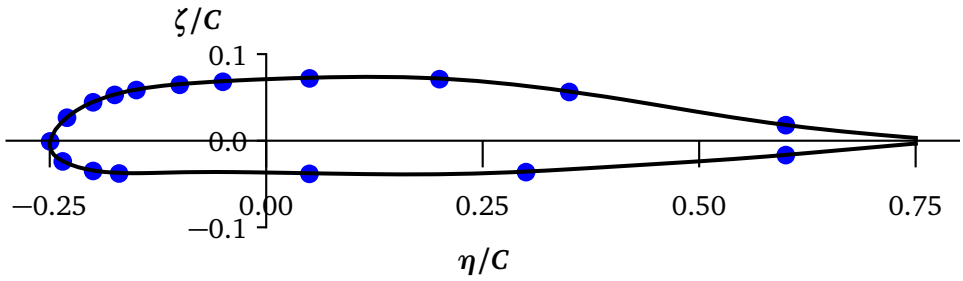

Figure 7. Station 3, Hover Blade - Kulite Locations.

Table 6. Station 3, Hover Blade - Nominal r/R: 0.673, Kulites 35 - 51.

Kulite ID	X (in)	Y (in)	Z (in)	r/R	η/c	ζ/c
35	44.588	-3.268	-0.155	0.670	0.600	-0.017
36	44.588	-1.631	-0.230	0.670	0.300	-0.036
37	44.588	-0.268	-0.214	0.670	0.050	-0.038
38	44.588	0.930	-0.188	0.670	-0.170	-0.038
39	44.588	1.093	-0.169	0.670	-0.200	-0.035
40	44.588	1.283	-0.105	0.670	-0.235	-0.024
41	44.888	-3.272	0.037	0.675	0.600	0.018
42	44.888	-1.913	0.271	0.675	0.350	0.056
43	44.888	-1.098	0.367	0.675	0.200	0.071
44	44.888	-0.280	0.387	0.675	0.050	0.072
45	44.888	0.266	0.376	0.675	-0.050	0.068
46	44.888	0.538	0.362	0.675	-0.100	0.065
47	44.888	0.811	0.334	0.675	-0.150	0.059
48	44.888	0.948	0.306	0.675	-0.175	0.053
49	44.888	1.085	0.262	0.675	-0.200	0.044
50	44.888	1.251	0.168	0.675	-0.230	0.027
51	44.888	1.360	0.021	0.675	-0.250	-0.001

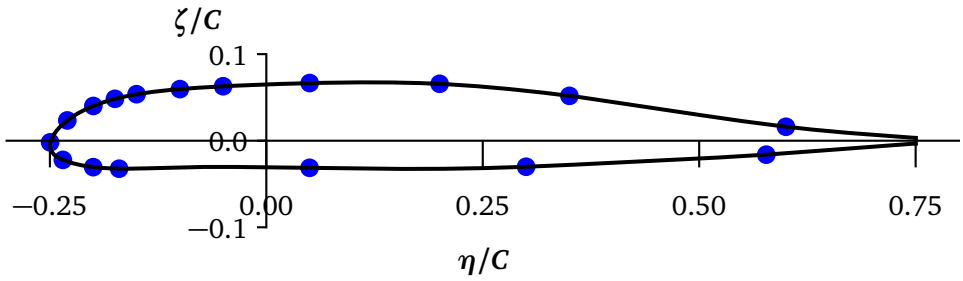

Figure 8. Station 4, Hover Blade - Kulite Locations.

Table 7. Station 4, Hover Blade - Nominal r/R: 0.748, Kulites 52 - 68.

Kulite ID	X (in)	Y (in)	Z (in)	r/R	η/c	ζ/c
52	49.575	-3.147	-0.092	0.745	0.577	-0.016
53	49.575	-1.635	-0.166	0.745	0.300	-0.030
54	49.575	-0.272	-0.171	0.745	0.050	-0.031
55	49.575	0.927	-0.175	0.745	-0.170	-0.032
56	49.575	1.090	-0.165	0.745	-0.200	-0.031
57	49.575	1.281	-0.119	0.745	-0.235	-0.022
58	49.875	1.361	-0.010	0.750	-0.250	-0.002
59	49.875	1.253	0.128	0.750	-0.230	0.023
60	49.875	1.089	0.219	0.750	-0.200	0.040
61	49.875	0.953	0.264	0.750	-0.175	0.048
62	49.875	0.817	0.293	0.750	-0.150	0.054
63	49.875	0.544	0.325	0.750	-0.100	0.060
64	49.875	0.272	0.343	0.750	-0.050	0.063
65	49.875	-0.273	0.363	0.750	0.050	0.067
66	49.875	-1.091	0.358	0.750	0.200	0.066
67	49.875	-1.908	0.282	0.750	0.350	0.052
68	49.875	-3.271	0.087	0.750	0.600	0.016

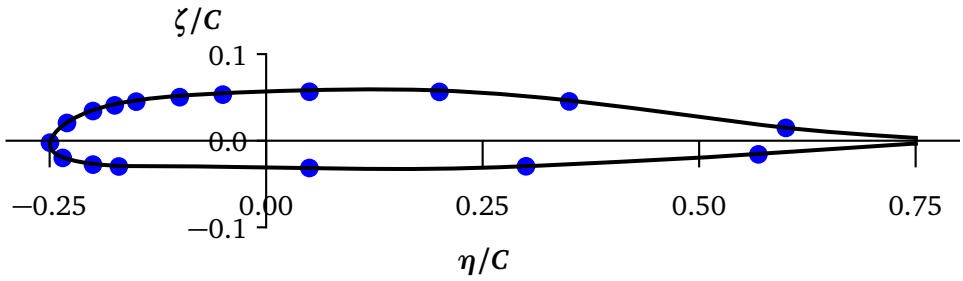

Figure 9. Station 5, Hover Blade - Kulite Locations.

Table 8. Station 5, Hover Blade - Nominal r/R: 0.823, Kulites 69 - 85.

Kulite ID	X (in)	Y (in)	Z (in)	r/R	η/c	ζ/c
69	54.563	-3.099	-0.033	0.820	0.568	-0.016
70	54.563	-1.638	-0.133	0.820	0.300	-0.030
71	54.563	-0.275	-0.167	0.820	0.050	-0.031
72	54.563	0.924	-0.178	0.820	-0.170	-0.030
73	54.563	1.087	-0.169	0.820	-0.200	-0.028
74	54.563	1.278	-0.130	0.820	-0.235	-0.020
75	54.863	-3.269	0.140	0.825	0.600	0.015
76	54.863	-1.903	0.282	0.825	0.350	0.045
77	54.863	-1.085	0.327	0.825	0.200	0.056
78	54.863	-0.267	0.313	0.825	0.050	0.057
79	54.863	0.278	0.285	0.825	-0.050	0.053
80	54.863	0.549	0.264	0.825	-0.100	0.050
81	54.863	0.822	0.231	0.825	-0.150	0.045
82	54.863	0.957	0.205	0.825	-0.175	0.041
83	54.863	1.093	0.167	0.825	-0.200	0.034
84	54.863	1.255	0.089	0.825	-0.230	0.021
85	54.863	1.360	-0.037	0.825	-0.250	-0.002

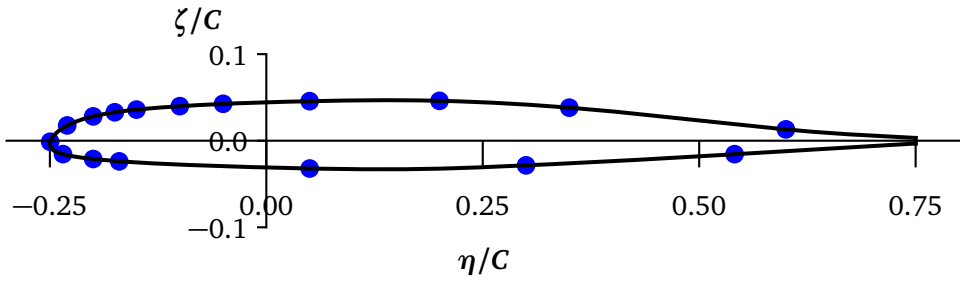

Figure 10. Station 6, Hover Blade - Kulite Locations.

Table 9. Station 6, Hover Blade - Nominal r/R: 0.873, Kulites 86 - 102.

Kulite ID	X (in)	Y (in)	Z (in)	r/R	η/c	ζ/c
86	57.888	-2.949	0.002	0.870	0.541	-0.016
87	57.888	-1.639	-0.107	0.870	0.300	-0.028
88	57.888	-0.278	-0.167	0.870	0.050	-0.032
89	57.888	0.922	-0.157	0.870	-0.170	-0.024
90	57.888	1.086	-0.147	0.870	-0.200	-0.021
91	57.888	1.277	-0.122	0.870	-0.235	-0.016
92	58.188	-3.267	0.171	0.875	0.600	0.013
93	58.188	-1.900	0.266	0.875	0.350	0.038
94	58.188	-1.082	0.284	0.875	0.200	0.046
95	58.188	-0.265	0.257	0.875	0.050	0.046
96	58.188	0.279	0.224	0.875	-0.050	0.043
97	58.188	0.551	0.201	0.875	-0.100	0.040
98	58.188	0.823	0.171	0.875	-0.150	0.036
99	58.188	0.959	0.150	0.875	-0.175	0.033
100	58.188	1.094	0.120	0.875	-0.200	0.028
101	58.188	1.256	0.058	0.875	-0.230	0.018
102	58.188	1.360	-0.048	0.875	-0.250	-0.001

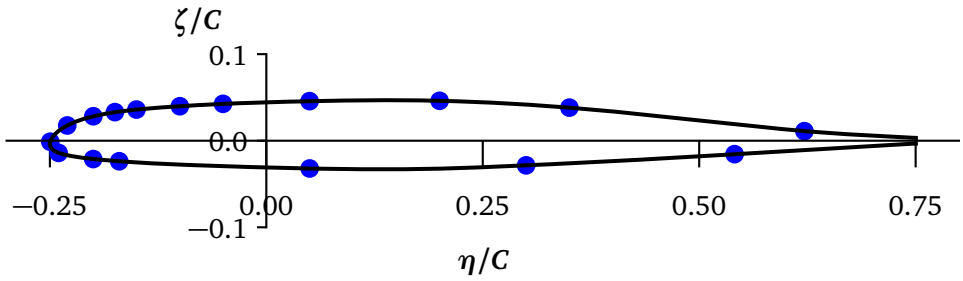

Figure 11. Station 7, Hover Blade - Kulite Locations.

Table 10. Station 7, Hover Blade - Nominal r/R: 0.898, Kulites 103 - 119.

Kulite ID	X (in)	Y (in)	Z (in)	r/R	η/c	ζ/c
103	59.550	-0.279	-0.165	0.895	0.050	-0.032
104	59.550	1.304	-0.123	0.895	-0.240	-0.014
105	59.550	1.085	-0.154	0.895	-0.200	-0.021
106	59.550	-2.949	0.020	0.895	0.541	-0.016
107	59.550	0.921	-0.162	0.895	-0.170	-0.024
108	59.550	-1.640	-0.097	0.895	0.300	-0.028
109	59.850	-3.383	0.184	0.900	0.622	0.011
110	59.850	-1.899	0.278	0.900	0.350	0.038
111	59.850	-1.081	0.291	0.900	0.200	0.046
112	59.850	-0.263	0.259	0.900	0.050	0.046
113	59.850	0.281	0.222	0.900	-0.050	0.043
114	59.850	0.552	0.197	0.900	-0.100	0.040
115	59.850	0.824	0.166	0.900	-0.150	0.036
116	59.850	0.959	0.145	0.900	-0.175	0.033
117	59.850	1.094	0.114	0.900	-0.200	0.028
118	59.850	1.256	0.050	0.900	-0.230	0.018
119	59.850	1.359	-0.056	0.900	-0.250	-0.001

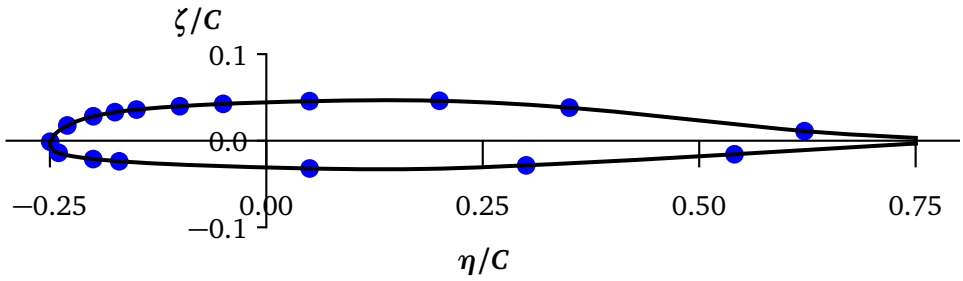

Figure 12. Station 8, Hover Blade - Kulite Locations.

Table 11. Station 8, Hover Blade - Nominal r/R: 0.928, Kulites 120 - 136.

Kulite ID	X (in)	Y (in)	Z (in)	r/R	η/c	ζ/c
120	61.545	0.920	-0.169	0.925	-0.170	-0.024
121	61.545	1.303	-0.132	0.925	-0.240	-0.014
122	61.545	1.084	-0.162	0.925	-0.200	-0.021
123	61.545	-0.280	-0.163	0.925	0.050	-0.032
124	61.545	-1.641	-0.085	0.925	0.300	-0.028
125	61.545	-2.948	0.041	0.925	0.541	-0.016
126	61.845	-3.382	0.209	0.930	0.622	0.011
127	61.845	-1.897	0.292	0.930	0.350	0.038
128	61.845	-1.078	0.299	0.930	0.200	0.046
129	61.845	-0.261	0.261	0.930	0.050	0.046
130	61.845	0.282	0.220	0.930	-0.050	0.043
131	61.845	0.554	0.193	0.930	-0.100	0.040
132	61.845	0.825	0.160	0.930	-0.150	0.036
133	61.845	0.960	0.138	0.930	-0.175	0.033
134	61.845	1.095	0.106	0.930	-0.200	0.028
135	61.845	1.256	0.041	0.930	-0.230	0.018
136	61.845	1.359	-0.066	0.930	-0.250	-0.001

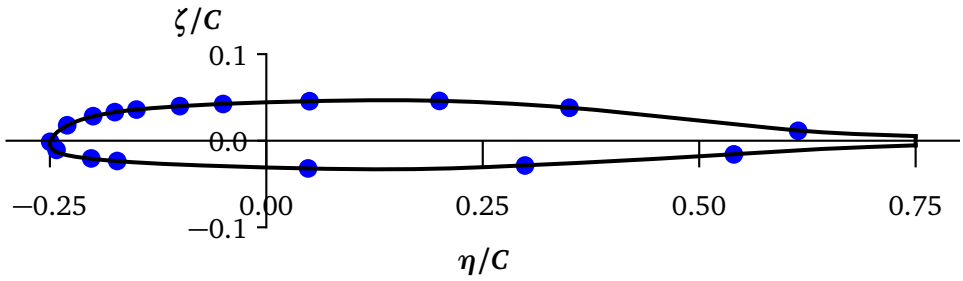

Figure 13. Station 9, Hover Blade - Kulite Locations.

Table 12. Station 9, Hover Blade - Nominal r/R: 0.953, Kulites 137 - 153.

Kulite ID	X (in)	Y (in)	Z (in)	r/R	η/c	ζ/c
137	63.208	1.303	-0.122	0.950	-0.242	-0.011
138	63.208	1.083	-0.165	0.950	-0.202	-0.020
139	63.208	0.919	-0.173	0.950	-0.172	-0.023
140	63.208	-0.281	-0.161	0.950	0.048	-0.032
141	63.208	-1.641	-0.076	0.950	0.299	-0.029
142	63.208	-2.948	0.058	0.950	0.540	-0.016
143	63.508	-3.396	0.221	0.955	0.614	0.011
144	63.508	-2.006	0.291	0.955	0.350	0.038
145	63.508	-1.218	0.293	0.955	0.200	0.046
146	63.508	-0.433	0.252	0.955	0.050	0.046
147	63.508	0.089	0.209	0.955	-0.050	0.042
148	63.508	0.350	0.183	0.955	-0.100	0.040
149	63.508	0.611	0.149	0.955	-0.150	0.036
150	63.508	0.741	0.127	0.955	-0.175	0.033
151	63.508	0.871	0.096	0.955	-0.200	0.028
152	63.508	1.025	0.033	0.955	-0.230	0.018
153	63.508	1.123	-0.072	0.955	-0.250	-0.001

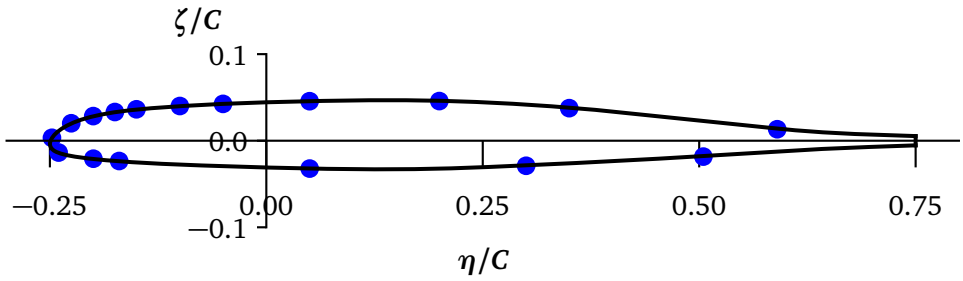

Figure 14. Station 10, Hover Blade - Kulite Locations.

Table 13. Station 10, Hover Blade - Nominal r/R: 0.971, Kulites 154 - 170.

Kulite ID	X (in)	Y (in)	Z (in)	r/R	η/c	ζ/c
154	64.405	-3.050	0.040	0.968	0.505	-0.018
155	64.405	-2.102	-0.060	0.968	0.300	-0.029
156	64.405	-0.942	-0.137	0.968	0.050	-0.032
157	64.405	0.082	-0.151	0.968	-0.170	-0.023
158	64.405	0.221	-0.146	0.968	-0.200	-0.021
159	64.405	0.409	-0.123	0.968	-0.240	-0.014
160	64.705	0.227	-0.045	0.973	-0.248	0.003
161	64.705	0.132	0.035	0.973	-0.225	0.020
162	64.705	0.021	0.078	0.973	-0.200	0.028
163	64.705	-0.089	0.105	0.973	-0.175	0.033
164	64.705	-0.199	0.125	0.973	-0.150	0.036
165	64.705	-0.421	0.154	0.973	-0.100	0.040
166	64.705	-0.642	0.177	0.973	-0.050	0.043
167	64.705	-1.086	0.215	0.973	0.050	0.046
168	64.705	-1.752	0.252	0.973	0.200	0.046
169	64.705	-2.421	0.252	0.973	0.350	0.038
170	64.705	-3.495	0.202	0.973	0.590	0.013

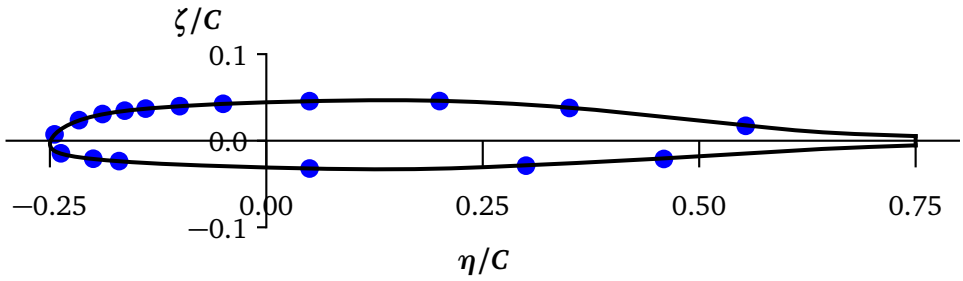

Figure 15. Station 11, Hover Blade - Kulite Locations.

Table 14. Station 11, Hover Blade - Nominal r/R: 0.988, Kulites 171 - 187.

Kulite ID	X (in)	Y (in)	Z (in)	r/R	η/c	ζ/c
171	65.535	-0.432	-0.110	0.985	-0.237	-0.015
172	65.535	-0.579	-0.126	0.985	-0.200	-0.021
173	65.535	-0.696	-0.130	0.985	-0.170	-0.024
174	65.535	-1.556	-0.114	0.985	0.050	-0.032
175	65.535	-2.530	-0.045	0.985	0.300	-0.029
176	65.535	-3.149	0.021	0.985	0.459	-0.021
177	65.835	-3.573	0.184	0.990	0.554	0.017
178	65.835	-2.815	0.216	0.990	0.350	0.038
179	65.835	-2.258	0.213	0.990	0.200	0.046
180	65.835	-1.702	0.180	0.990	0.050	0.046
181	65.835	-1.333	0.147	0.990	-0.050	0.043
182	65.835	-1.148	0.126	0.990	-0.100	0.040
183	65.835	-1.003	0.107	0.990	-0.139	0.037
184	65.835	-0.914	0.093	0.990	-0.164	0.035
185	65.835	-0.820	0.073	0.990	-0.189	0.031
186	65.835	-0.721	0.041	0.990	-0.216	0.024
187	65.835	-0.620	-0.026	0.990	-0.245	0.007

3.1.2 Acoustic Blade, SN006 Pressures

The Acoustic Blade, SN006, was instrumented with 51 absolute dynamic pressure transducers distributed in two triangular patterns near the leading edge, centered about $r/R = 0.75$ and $r/R = 0.90$, as shown by Figure 4. The predesign layout for the pressure transducers on the Acoustic Blade was influenced by the transducer layout on other acoustic rotor test blades, most notably the transducer layout on the HART II blade [6]. The predesign layout spacing had to be modified in the design phase in order to accommodate the physical size of the transducers and wiring.

The pressure transducer locations, in both global coordinates and nondimensional coordinates, are provided in Tables 15-16.

Table 15. Acoustic Blade - Locations of Kulites 1 - 17.

Kulite ID	X (in)	Y (in)	Z (in)	r/R	η/c	ζ/c
188	48.375	1.199	-0.140	0.727	-0.220	-0.027
189	48.375	1.198	0.172	0.727	-0.220	0.030
190	49.125	1.199	-0.143	0.739	-0.220	-0.027
191	49.125	1.198	0.168	0.739	-0.220	0.030
192	49.125	1.035	0.242	0.739	-0.190	0.044
193	49.875	1.199	-0.147	0.750	-0.220	-0.027
194	49.875	1.036	-0.171	0.750	-0.190	-0.031
195	49.875	0.872	-0.176	0.750	-0.160	-0.032
196	49.875	1.198	0.165	0.750	-0.220	0.030
197	49.875	1.035	0.239	0.750	-0.190	0.044
198	49.875	0.871	0.282	0.750	-0.160	0.052
199	50.625	1.198	-0.150	0.761	-0.220	-0.027
200	50.625	1.035	-0.174	0.761	-0.190	-0.031
201	50.625	1.199	0.162	0.761	-0.220	0.030
202	50.625	1.036	0.236	0.761	-0.190	0.044
203	51.375	1.198	-0.153	0.773	-0.220	-0.027
204	51.375	1.199	0.159	0.773	-0.220	0.030

Table 16. Acoustic Blade - Locations of Kulites 18 - 51.

Kulite ID	X (in)	Y (in)	Z (in)	r/R	η/c	ζ/c
205	56.850	1.195	-0.132	0.855	-0.220	-0.019
206	56.850	1.201	0.090	0.855	-0.220	0.022
207	57.600	1.195	-0.135	0.866	-0.220	-0.019
208	57.600	1.201	0.087	0.866	-0.220	0.022
209	58.350	1.195	-0.139	0.877	-0.220	-0.019
210	58.350	1.031	-0.153	0.877	-0.190	-0.022
211	58.350	1.202	0.083	0.877	-0.220	0.022
212	58.350	1.040	0.133	0.877	-0.190	0.030
213	59.100	1.194	-0.142	0.889	-0.220	-0.019
214	59.100	1.031	-0.155	0.889	-0.190	-0.022
215	59.100	0.867	-0.163	0.889	-0.160	-0.025
216	59.100	1.202	0.080	0.889	-0.220	0.022
217	59.100	1.040	0.130	0.889	-0.190	0.030
218	59.100	0.877	0.161	0.889	-0.160	0.035
219	59.850	1.194	-0.145	0.900	-0.220	-0.019
220	59.850	1.031	-0.158	0.900	-0.190	-0.022
221	59.850	0.866	-0.165	0.900	-0.160	-0.024
222	59.850	0.703	-0.169	0.900	-0.130	-0.026
223	59.850	1.202	0.077	0.900	-0.220	0.022
224	59.850	1.041	0.128	0.900	-0.190	0.030
225	59.850	0.878	0.158	0.900	-0.160	0.035
226	59.850	0.715	0.180	0.900	-0.130	0.038
227	59.850	0.389	0.213	0.900	-0.070	0.042
228	60.600	1.194	-0.148	0.911	-0.220	-0.019
229	60.600	1.030	-0.161	0.911	-0.190	-0.022
230	60.600	1.202	0.073	0.911	-0.220	0.022
231	60.600	1.041	0.125	0.911	-0.190	0.030
232	61.350	1.193	-0.152	0.923	-0.220	-0.019
233	61.350	1.202	0.070	0.923	-0.220	0.022
234	61.350	1.041	0.122	0.923	-0.190	0.030
235	62.100	1.193	-0.155	0.934	-0.220	-0.019
236	62.100	1.202	0.067	0.934	-0.220	0.022
237	62.850	1.193	-0.158	0.945	-0.220	-0.019
238	62.850	1.202	0.064	0.945	-0.220	0.022

3.2 Strain Gauges

All of the blades, SN001-006, were instrumented with full-bridge flap, chord and torsion strain gauges at the root. Blade SN005, Strain Blade, was instrumented with four additional sets of flap, chord and torsion gauges. They are calibrated with reference to their radial station, X, and $Y = 0$, $Z = 0$ in an untwisted reference frame. A 3x3 calibration matrix is utilized to minimize the cross-coupling between the gauges. The spanwise location of the gauges is provided in Table 17.

Table 17. Radial Locations of the Strain Gauge Bridges per Blade Serial Number.

r/R	X (in)	Flap	Chord	Torsion
0.253	26.72	001-006	001-006	-
0.261	27.33	-	-	001-006
0.423	28.10	005	005	-
0.430	28.60	-	-	005
0.611	40.65	005	005	-
0.619	41.15	-	-	005
0.836	55.61	005	005	-
0.844	56.11	-	-	005

3.3 Temperature Sensors

All of the blades had seven Resistance Temperature Detectors (RTD) installed along the radius at the local $\eta/c = 0.50$ to measure local temperature. The sensors were installed in the foam midway between the upper and lower surface skin. The radial locations of the RTDs are provided in Table 18.

Table 18. Radial Locations of RTDs.

r/R	X (in)
0.402	26.72
0.506	33.62
0.609	40.51
0.713	47.40
0.808	53.76
0.896	59.59
0.972	64.67

3.4 Tip Tracking LEDs

All of the blades had an LED installed at the local quarter-chord, $\eta/c = 0.0$, of the tip to be used for blade tracking.

4 Structural Properties

The 2D sectional properties of the blade were calculated using VABS3.8 [7]. The properties are calculated using the Timoshenko model, where the sectional stiffnesses are reported about the tension center, and the Vlasov model, where the sectional stiffnesses are reported about the shear center. In both models, the mass properties are reported both about the shear center and about the local center of gravity (CG). The shear center (SC_η, SC_ζ), center of gravity (CG_η, CG_ζ), and tension center ($\bar{\eta}, \bar{\zeta}$) are reported relative to local η, ζ coordinate system. Note that the local coordinate system is untwisted and the structure properties are also provided in the untwisted reference frame. The input and output VABS files, which include the full 6x6 mass and stiffness matrices, are available upon request.

Two sets of blade sectional properties were developed: (1) Hover Blade Properties, see Section 4.1, and (2) the Acoustic Blade Properties, see Section 4.2. Blade SN001-005, which includes the Standard, Hover and Strain Blade, should use the Hover Blade Properties. The Acoustic Blade Properties should only be used with the Acoustic Blade (SN006). The difference in properties was due to the different instrumentation requirements.

4.1 Hover Blade Properties

Table 19. Blade Sectional Properties for Blades SN001-SN005 (Hover Set).

r/R	ρA $lbf \cdot s^2/in^2$	EA lbf	$GJ@SC$ $lbf \cdot in^2$	SC_η in	SC_ζ in	CG_η in	CG_ζ in	$\bar{\eta}$ in	$\bar{\zeta}$ in
0.178	2.980E-04	1.300E+07	2.740E+05	0.127	0.012	1.279	-0.027	-0.001	-0.002
0.215	2.190E-04	7.380E+06	2.360E+05	-0.002	0.054	-0.017	0.031	-0.052	0.040
0.252	2.060E-04	6.280E+06	2.140E+05	0.031	0.112	-0.050	0.056	-0.051	0.078
0.389	1.580E-04	6.190E+06	1.690E+05	0.081	0.134	0.665	0.056	-0.026	0.112
0.405	1.570E-04	6.190E+06	1.680E+05	0.089	0.091	0.660	0.097	-0.025	0.047
0.469	2.040E-04	5.780E+06	2.140E+05	0.033	0.113	-0.040	0.055	-0.051	0.078
0.529	2.000E-04	5.190E+06	2.160E+05	0.040	0.112	-0.049	0.055	-0.031	0.078
0.595	2.160E-04	4.730E+06	1.150E+05	0.118	0.114	-0.055	0.069	0.086	0.084
0.600	2.190E-04	4.740E+06	1.160E+05	0.118	0.119	0.005	0.062	0.087	0.085
0.608	2.450E-04	4.730E+06	1.150E+05	0.120	0.114	-0.233	0.052	0.085	0.084
0.676	2.220E-04	4.480E+06	8.610E+04	0.150	0.112	-0.277	0.048	0.126	0.085
0.676	1.930E-04	4.480E+06	8.620E+04	0.151	0.110	-0.088	0.065	0.127	0.085
0.676	1.900E-04	4.480E+06	8.650E+04	0.150	0.113	-0.041	0.052	0.127	0.086
0.701	2.060E-04	4.240E+06	6.470E+04	0.279	0.108	-0.264	0.047	0.175	0.087
0.745	1.790E-04	4.240E+06	6.470E+04	0.281	0.108	-0.035	0.065	0.176	0.087
0.750	1.770E-04	4.250E+06	6.500E+04	0.280	0.110	0.012	0.053	0.176	0.087
0.826	2.140E-04	3.670E+06	4.200E+04	0.218	0.078	-0.316	0.034	0.218	0.061
0.826	1.790E-04	3.670E+06	4.210E+04	0.220	0.077	-0.096	0.051	0.219	0.061
0.826	1.800E-04	3.680E+06	4.230E+04	0.220	0.080	-0.064	0.034	0.219	0.061
0.851	2.120E-04	3.110E+06	2.730E+04	0.315	0.061	-0.336	0.023	0.260	0.035
0.925	1.710E-04	3.110E+06	2.730E+04	0.317	0.060	-0.094	0.038	0.261	0.035
0.920	1.840E-04	3.130E+06	2.750E+04	0.323	0.055	0.025	0.029	0.267	0.034
0.930	1.740E-04	3.120E+06	2.760E+04	0.328	0.061	-0.070	0.018	0.261	0.035
0.936	1.880E-04	3.130E+06	2.790E+04	0.344	0.066	0.077	0.027	0.268	0.036
0.990	5.600E-05	1.290E+06	4.120E+03	1.587	0.033	1.889	0.017	1.825	0.023
0.990	5.940E-05	1.290E+06	4.140E+03	1.590	0.035	1.896	0.024	1.825	0.024
0.998	4.280E-05	9.530E+05	2.530E+03	2.249	0.028	2.385	0.017	2.257	0.020

Table 20. Timoshenko Model Blade Section Properties for Blades SN001-SN005 (Hover Set).

	About the Neutral Axis $(\bar{\eta}, \bar{\zeta})$			About the CG (CG_η, CG_ζ)		
r/R	EI_F $lbf \cdot in^2$	EI_C $lbf \cdot in^2$	EI_{FC} $lbf \cdot in^2$	I_F $lbf \cdot s^2 \cdot in$	I_C $lbf \cdot s^2 \cdot in$	I_{FC} $lbf \cdot s^2 \cdot in$
0.178	288859	7.070E+06	3.300E+04	7.200E-06	9.060E-04	1.620E-05
0.215	308234	4.540E+06	-1.990E+04	6.160E-06	3.630E-04	-1.880E-06
0.252	345802	4.030E+06	-5.560E+04	6.750E-06	3.360E-04	-5.930E-06
0.389	259208	3.930E+06	-1.950E+04	6.540E-06	2.620E-04	2.820E-06
0.405	258124	3.920E+06	-6.970E+04	6.430E-06	2.630E-04	-1.150E-06
0.469	323093	3.890E+06	-5.180E+04	6.500E-06	3.430E-04	-5.590E-06
0.529	296044	3.600E+06	-4.230E+04	6.500E-06	3.340E-04	-5.880E-06
0.595	148270	2.940E+06	-7.010E+03	5.490E-06	3.740E-04	-1.850E-06
0.600	148925	2.940E+06	-9.080E+03	6.830E-06	3.720E-04	-1.090E-05
0.608	148135	2.920E+06	-7.940E+03	6.110E-06	3.940E-04	-7.670E-06
0.676	107293	2.610E+06	5.730E+03	4.570E-06	3.420E-04	-4.170E-06
0.676	107422	2.620E+06	6.540E+03	4.060E-06	3.250E-04	8.380E-07
0.676	107602	2.630E+06	5.550E+03	4.950E-06	3.250E-04	-6.670E-06
0.701	74230	2.370E+06	1.170E+04	3.530E-06	3.250E-04	-4.040E-06
0.745	74337	2.380E+06	1.240E+04	3.100E-06	3.060E-04	6.760E-07
0.750	74471	2.380E+06	1.160E+04	3.680E-06	3.000E-04	-4.930E-06
0.826	44624	2.120E+06	1.100E+04	2.480E-06	3.170E-04	-2.160E-06
0.826	44702	2.130E+06	1.150E+04	2.140E-06	2.980E-04	1.960E-06
0.826	44820	2.140E+06	1.090E+04	2.530E-06	2.970E-04	-4.030E-06
0.851	24143	1.890E+06	7.400E+03	1.630E-06	3.010E-04	-5.930E-07
0.925	24198	1.900E+06	7.820E+03	1.420E-06	2.800E-04	2.820E-06
0.920	24427	1.930E+06	9.770E+03	1.650E-06	3.220E-04	5.290E-06
0.930	24293	1.900E+06	7.390E+03	1.610E-06	2.830E-04	-2.870E-06
0.936	24492	1.950E+06	5.840E+03	1.860E-06	3.440E-04	-5.180E-06
0.990	2903	4.380E+05	3.070E+03	2.670E-07	5.240E-05	5.180E-07
0.990	2925	4.410E+05	2.980E+03	2.990E-07	5.440E-05	3.010E-08
0.998	1616	2.600E+05	1.370E+03	1.790E-07	2.950E-05	1.220E-07

Table 21. Vlasov Model Blade Section Properties for Blades SN001-SN005 (Hover Set).

	About the Shear Center (SC_η, SC_ζ)					
r/R	EI_F $lbf \cdot in^2$	EI_C $lbf \cdot in^2$	EI_{FC} $lbf \cdot in^2$	I_F $lbf \cdot s^2 \cdot in$	I_C $lbf \cdot s^2 \cdot in$	I_{FC} $lbf \cdot s^2 \cdot in$
0.178	2.910E+05	7.290E+06	9.450E+03	7.990E-06	1.320E-03	3.420E-05
0.215	3.100E+05	4.560E+06	-2.500E+04	6.270E-06	3.630E-04	-1.960E-06
0.252	3.530E+05	4.080E+06	-7.260E+04	7.390E-06	3.370E-04	-6.850E-06
0.389	2.620E+05	4.000E+06	-3.440E+04	7.510E-06	3.160E-04	1.000E-05
0.405	2.700E+05	4.000E+06	-1.010E+05	6.440E-06	3.140E-04	-1.640E-06
0.469	3.300E+05	3.930E+06	-6.870E+04	7.180E-06	3.440E-04	-6.460E-06
0.529	3.020E+05	3.630E+06	-5.490E+04	7.150E-06	3.350E-04	-6.900E-06
0.595	1.530E+05	2.940E+06	-1.160E+04	5.920E-06	3.810E-04	-3.540E-06
0.600	1.550E+05	2.950E+06	-1.410E+04	7.540E-06	3.740E-04	-1.230E-05
0.608	1.520E+05	2.930E+06	-1.280E+04	7.060E-06	4.240E-04	-1.300E-05
0.676	1.100E+05	2.610E+06	2.850E+03	5.470E-06	3.830E-04	-1.020E-05
0.676	1.100E+05	2.630E+06	3.820E+03	4.450E-06	3.360E-04	-1.230E-06
0.676	1.110E+05	2.630E+06	2.660E+03	5.450E-06	3.260E-04	-7.820E-06
0.701	7.620E+04	2.410E+06	2.150E+03	4.290E-06	3.790E-04	-1.050E-05
0.745	7.620E+04	2.420E+06	3.040E+03	3.430E-06	3.240E-04	-1.750E-06
0.750	7.680E+04	2.430E+06	1.450E+03	4.250E-06	3.130E-04	-7.620E-06
0.826	4.570E+04	2.120E+06	1.100E+04	2.890E-06	3.780E-04	-7.170E-06
0.826	4.560E+04	2.130E+06	1.150E+04	2.250E-06	3.160E-04	5.080E-07
0.826	4.610E+04	2.140E+06	1.090E+04	2.910E-06	3.120E-04	-6.360E-06
0.851	2.630E+04	1.900E+06	2.960E+03	1.930E-06	3.900E-04	-5.820E-06
0.925	2.620E+04	1.910E+06	3.430E+03	1.500E-06	3.090E-04	1.260E-06
0.920	2.570E+04	1.940E+06	6.170E+03	1.770E-06	3.390E-04	3.860E-06
0.930	2.630E+04	1.920E+06	2.090E+03	1.920E-06	3.110E-04	-5.800E-06
0.936	2.730E+04	1.970E+06	-1.300E+03	2.140E-06	3.570E-04	-7.110E-06
0.990	3.030E+03	5.110E+05	6.060E+03	2.800E-07	5.750E-05	7.780E-07
0.990	3.090E+03	5.120E+05	6.350E+03	3.050E-07	5.990E-05	2.210E-07
0.998	1.670E+03	2.600E+05	1.410E+03	1.840E-07	3.030E-05	1.830E-07

4.2 Acoustic Blade Properties

Table 22. Blade Sectional Properties for the Acoustic Blade (SN006).

r/R	ρA $lbf \cdot s^2/in^2$	EA lbf	$GJ@SC$ $lbf \cdot in^2$	SC_η in	SC_ζ in	CG_η in	CG_ζ in	$\bar{\eta}$ in	$\bar{\zeta}$ in
0.178	2.980E-04	1.300E+07	2.740E+05	0.127	0.012	1.279	-0.027	-0.001	-0.002
0.215	2.190E-04	7.380E+06	2.360E+05	-0.002	0.054	-0.017	0.031	-0.052	0.040
0.252	2.060E-04	6.280E+06	2.140E+05	0.031	0.112	-0.050	0.056	-0.051	0.078
0.389	1.580E-04	6.190E+06	1.690E+05	0.081	0.134	0.665	0.056	-0.026	0.112
0.405	1.570E-04	6.190E+06	1.680E+05	0.089	0.091	0.660	0.097	-0.025	0.047
0.469	2.040E-04	5.780E+06	2.140E+05	0.033	0.113	-0.040	0.055	-0.051	0.078
0.529	2.000E-04	5.190E+06	2.160E+05	0.040	0.112	-0.049	0.055	-0.031	0.078
0.595	2.380E-04	4.730E+06	1.150E+05	0.120	0.114	-0.169	0.050	0.086	0.084
0.600	2.490E-04	4.740E+06	1.160E+05	0.119	0.119	-0.145	0.067	0.087	0.085
0.608	2.350E-04	4.730E+06	1.150E+05	0.120	0.114	-0.197	0.052	0.085	0.084
0.676	2.080E-04	4.480E+06	8.640E+04	0.146	0.111	-0.223	0.049	0.126	0.085
0.676	2.110E-04	4.480E+06	8.650E+04	0.146	0.109	-0.193	0.047	0.127	0.085
0.676	2.150E-04	4.480E+06	8.690E+04	0.145	0.113	-0.186	0.057	0.127	0.086
0.701	2.380E-04	4.240E+06	6.480E+04	0.278	0.108	-0.344	0.046	0.175	0.087
0.745	1.670E-04	4.240E+06	6.440E+04	0.281	0.192	0.004	0.059	0.175	0.087
0.826	2.000E-04	3.670E+06	4.200E+04	0.221	0.078	-0.269	0.035	0.218	0.061
0.826	2.040E-04	3.670E+06	4.210E+04	0.222	0.077	-0.237	0.033	0.219	0.061
0.826	2.080E-04	3.680E+06	4.230E+04	0.221	0.080	-0.228	0.041	0.219	0.061
0.851	2.710E-04	3.110E+06	2.740E+04	0.310	0.061	-0.441	0.025	0.260	0.035
0.900	1.620E-04	3.110E+06	2.720E+04	0.313	0.061	-0.037	0.029	0.260	0.035
0.925	2.740E-04	3.120E+06	2.760E+04	0.314	0.061	-0.415	0.023	0.262	0.035
0.920	2.870E-04	3.130E+06	2.770E+04	0.317	0.055	-0.324	0.018	0.267	0.034
0.930	2.790E-04	3.120E+06	2.780E+04	0.323	0.061	-0.405	0.028	0.261	0.035
0.936	2.930E-04	3.130E+06	2.810E+04	0.339	0.066	-0.294	0.034	0.269	0.036
0.990	6.560E-05	1.290E+06	4.160E+03	1.623	0.032	1.711	0.012	1.825	0.023
0.990	6.960E-05	1.290E+06	4.270E+03	1.681	0.034	1.717	0.024	1.825	0.024
0.998	4.910E-05	9.530E+05	2.530E+03	2.255	0.028	2.237	0.016	2.257	0.020

Table 23. Timoshenko Model Blade Section Properties for the Acoustic Blade (SN006).

	About the Neutral Axis $(\bar{\eta}, \bar{\zeta})$			About the CG (CG_η, CG_ζ)		
r/R	EI_F $lbf \cdot in^2$	EI_C $lbf \cdot in^2$	EI_{FC} $lbf \cdot in^2$	I_F $lbf \cdot s^2 \cdot in$	I_C $lbf \cdot s^2 \cdot in$	I_{FC} $lbf \cdot s^2 \cdot in$
0.178	288859	7.070E+06	3.300E+04	7.200E-06	9.060E-04	1.620E-05
0.215	308234	4.540E+06	-1.990E+04	6.160E-06	3.630E-04	-1.880E-06
0.252	345802	4.030E+06	-5.560E+04	6.750E-06	3.360E-04	-5.930E-06
0.389	259208	3.930E+06	-1.950E+04	6.540E-06	2.620E-04	2.820E-06
0.405	258124	3.920E+06	-6.970E+04	6.430E-06	2.630E-04	-1.150E-06
0.469	323093	3.890E+06	-5.180E+04	6.500E-06	3.430E-04	-5.590E-06
0.529	296044	3.600E+06	-4.230E+04	6.500E-06	3.340E-04	-5.880E-06
0.595	148269	2.930E+06	-7.000E+03	6.090E-06	4.040E-04	-6.540E-06
0.600	148923	2.940E+06	-9.070E+03	6.970E-06	4.130E-04	-9.780E-06
0.608	148112	2.920E+06	-7.920E+03	5.970E-06	3.860E-04	-7.470E-06
0.676	107290	2.610E+06	5.700E+03	5.140E-06	3.640E-04	-4.540E-06
0.676	107419	2.620E+06	6.520E+03	5.220E-06	3.830E-04	-3.650E-06
0.676	107599	2.630E+06	5.530E+03	5.560E-06	3.880E-04	-5.750E-06
0.701	74221	2.370E+06	1.160E+04	4.520E-06	3.600E-04	-4.470E-06
0.745	74221	2.370E+06	1.160E+04	3.180E-06	3.010E-04	-2.100E-06
0.826	44621	2.120E+06	1.100E+04	2.740E-06	3.290E-04	-2.170E-06
0.826	44699	2.130E+06	1.150E+04	2.800E-06	3.470E-04	-1.470E-06
0.826	44817	2.140E+06	1.090E+04	3.000E-06	3.530E-04	-3.110E-06
0.851	24138	1.890E+06	7.410E+03	1.890E-06	3.120E-04	-4.570E-07
0.900	24138	1.890E+06	7.410E+03	1.270E-06	2.440E-04	3.840E-07
0.925	24213	1.900E+06	7.830E+03	1.950E-06	3.370E-04	1.170E-07
0.920	24422	1.930E+06	9.770E+03	2.130E-06	3.880E-04	2.890E-06
0.930	24288	1.900E+06	7.390E+03	2.060E-06	3.380E-04	-1.250E-06
0.936	24487	1.950E+06	5.840E+03	2.280E-06	4.190E-04	-3.870E-06
0.990	2903	4.380E+05	3.070E+03	2.710E-07	6.440E-05	1.720E-07
0.990	2925	4.410E+05	2.980E+03	3.020E-07	6.730E-05	-1.610E-08
0.998	1616	2.600E+05	1.370E+03	1.810E-07	3.690E-05	6.130E-08

Table 24. Vlasov Model Blade Section Properties for the Acoustic Blade (SN006).

	About the Shear Center (SC_η, SC_ζ)					
r/R	EI_F $lbf \cdot in^2$	EI_C $lbf \cdot in^2$	EI_{FC} $lbf \cdot in^2$	I_F $lbf \cdot s^2 \cdot in$	I_C $lbf \cdot s^2 \cdot in$	I_{FC} $lbf \cdot s^2 \cdot in$
0.178	2.910E+05	7.290E+06	9.450E+03	7.990E-06	1.320E-03	3.420E-05
0.215	3.100E+05	4.560E+06	-2.500E+04	6.270E-06	3.630E-04	-1.960E-06
0.252	3.530E+05	4.080E+06	-7.260E+04	7.390E-06	3.370E-04	-6.850E-06
0.389	2.620E+05	4.000E+06	-3.440E+04	7.510E-06	3.160E-04	1.000E-05
0.405	2.700E+05	4.000E+06	-1.010E+05	6.440E-06	3.140E-04	-1.640E-06
0.469	3.300E+05	3.930E+06	-6.870E+04	7.180E-06	3.440E-04	-6.460E-06
0.529	3.020E+05	3.630E+06	-5.490E+04	7.150E-06	3.350E-04	-6.900E-06
0.595	1.530E+05	2.940E+06	-1.180E+04	7.060E-06	4.240E-04	-1.100E-05
0.600	1.550E+05	2.950E+06	-1.440E+04	6.970E-06	4.130E-04	-9.780E-06
0.608	1.520E+05	2.930E+06	-1.280E+04	6.860E-06	4.100E-04	-1.210E-05
0.676	1.100E+05	2.610E+06	3.400E+03	6.270E-06	4.440E-04	-1.410E-05
0.676	1.100E+05	2.630E+06	4.450E+03	6.380E-06	4.570E-04	-1.290E-05
0.676	8.690E+04	2.630E+06	3.310E+03	6.580E-06	4.600E-04	-1.430E-05
0.701	7.620E+04	2.410E+06	2.160E+03	5.700E-06	5.220E-04	-1.830E-05
0.745	7.620E+04	2.410E+06	1.950E+03	3.730E-06	3.420E-04	-6.860E-06
0.826	4.570E+04	2.120E+06	1.080E+04	3.220E-06	4.250E-04	-8.920E-06
0.826	4.560E+04	2.130E+06	1.140E+04	3.280E-06	4.360E-04	-8.040E-06
0.826	4.610E+04	2.140E+06	1.080E+04	3.420E-06	4.400E-04	-9.120E-06
0.851	2.630E+04	1.890E+06	3.330E+03	2.260E-06	4.640E-04	-7.940E-06
0.900	2.630E+04	1.890E+06	3.090E+03	1.440E-06	2.630E-04	-1.460E-06
0.925	2.630E+04	1.910E+06	3.600E+03	2.340E-06	4.780E-04	-7.290E-06
0.920	2.580E+04	1.930E+06	6.540E+03	2.530E-06	5.060E-04	-3.960E-06
0.930	2.630E+04	1.910E+06	2.500E+03	2.350E-06	4.850E-04	-7.810E-06
0.936	2.740E+04	1.960E+06	-8.150E+02	2.580E-06	5.370E-04	-9.850E-06
0.990	3.010E+03	4.910E+05	5.470E+03	2.980E-07	6.500E-05	2.900E-07
0.990	3.070E+03	4.680E+05	4.910E+03	3.090E-07	6.740E-05	9.660E-09
0.998	1.670E+03	2.600E+05	1.380E+03	1.880E-07	3.690E-05	5.100E-08

References

1. Wong, O. D.; Noonan, K. W.; Watkins, A. N.; Jenkins, L. N.; and Yao, C. S.: Non-Intrusive Measurements of a Four-Bladed Rotor in Hover, A First Look. *American Helicopter Society Aeromechanics Specialists Conference*, San Francisco, CA, January 2010.

2. Overmeyer, A.; and Martin, P.: Measured Boundary Layer Transition and Hover Performance at Model Scale. *55th AIAA Aerospace Sciences Meeting*, Grapevine, TX, January 2017. AIAA 2017-1872.

3. Noonan, K.: Aerodynamic characteristics of two rotorcraft airfoils designed for application to the inboard region of a main rotor blade. *NASA-TP-3009, AVSCOM-TR-90-B-005*, NASA Langley Research Center, July 1990.

4. Noonan, K.: Aerodynamic characteristics of two rotorcraft airfoils designed for the tip region of a main rotor blade. *NASA-TM-4264,AVSCOM-TR-91-B-003*, NASA Langley Research Center, May 1991.

5. Eppler, R.; and Somers, D. M.: A Computer Program for the Design and Analysis of Low-Speed Airfoils. *NASA TM- 80210*, NASA Langley Research Center, August 1980.

6. van der Wall, B. G.: A comprehensive rotary-wing data base for code validation: The HART II International Workshop. *Aeronautical Journal*, vol. 115, no. 1164, 2011, pp. 91–102.

7. Cesnik, C. E.; and Hodges, D. H.: VABS: a new concept for composite rotor blade cross-sectional modeling. *Journal of the American Helicopter Society*, vol. 42, no. 1, 1997, pp. 27–38.

REPORT DOCUMENTATION PAGE

Form Approved
OMB No. 0704–0188

1. REPORT DATE *(DD-MM-YYYY)*	2. REPORT TYPE	3. DATES COVERED *(From - To)*
01-05-2020	Technical Memorandum	

4. TITLE AND SUBTITLE
Hover Validation and Acoustic Baseline Blade Set Definition

5a. CONTRACT NUMBER

5b. GRANT NUMBER

5c. PROGRAM ELEMENT NUMBER

6. AUTHOR(S)
Austin D. Overmeyer, Peter A. Copp Norman W. Schaeffler

5d. PROJECT NUMBER

5e. TASK NUMBER

5f. WORK UNIT NUMBER

7. PERFORMING ORGANIZATION NAME(S) AND ADDRESS(ES)
NASA Langley Research Center
Hampton, Virginia 23681-2199

8. PERFORMING ORGANIZATION REPORT NUMBER
L–

9. SPONSORING/MONITORING AGENCY NAME(S) AND ADDRESS(ES)
National Aeronautics and Space Administration
Washington, DC 20546-0001

10. SPONSOR/MONITOR'S ACRONYM(S)
NASA

11. SPONSOR/MONITOR'S REPORT NUMBER(S)
NASA/TM–2020–5002153

12. DISTRIBUTION/AVAILABILITY STATEMENT
Unclassified-Unlimited, Distribution Statement A: Approved for public release. CCDC AvMC PR20200157
Subject Category 02
Availability: NASA STI Program (757) 864-9658

13. SUPPLEMENTARY NOTES
An electronic version can be found at http://ntrs.nasa.gov.

14. ABSTRACT

The Hover Validation and Acoustic Baseline (HVAB) blade set has been jointly developed by the U.S. Army Combat Capabilities Development Command Aviation & Missile Center (CCDC AvMC) and the NASA Revolutionary Vertical Lift Technology (RVLT) Project. This Mach-scale, 66.50 *in* radius, blade set will ultimately be tested in both hover and forward-flight to provide key data for analysis validation. This paper provides comprehensive detail of the blade geometry, instrumentation, and structure for use in future analyses.

15. SUBJECT TERMS
Hover, Rotor, Helicopter, Validation, HVAB, PSP, Aerodynamics

16. SECURITY CLASSIFICATION OF:			17. LIMITATION OF ABSTRACT	18. NUMBER OF PAGES	19a. NAME OF RESPONSIBLE PERSON
a. REPORT	b. ABSTRACT	c. THIS PAGE			STI Information Desk (email: help@sti.nasa.gov)
U	U	U	UU	44	19b. TELEPHONE NUMBER *(Include area code)* (757) 864-9658